

**Burst pressure estimation of corroded pipeline
with interacting defects using FEA**

by

Ahmad Shakir bin Aminudin

Dissertation submitted in partial fulfillment of
the requirements for the
Bachelor of Engineering (Hons)
(Mechanical Engineering)

September 2011

Universiti Teknologi PETRONAS
Bandar Seri Iskandar
31750 Tronoh
Perak Darul Ridzuan

CERTIFICATION OF APPROVAL

**Burst pressure estimation of corroded pipeline
with interacting defects using FEA**

by

Ahmad Shakir bin Aminudin (10606)

A Project Dissertation submitted in partial fulfilment of

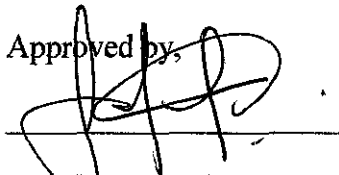
the requirements for the

Bachelor of Engineering (Hons)

(Mechanical Engineering)

SEPTEMBER 2011

Approved by,



(Dr. Saravanan Karuppanan)

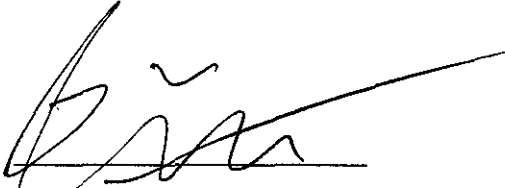
UNIVERSITI TEKNOLOGI PETRONAS

TRONOH, PERAK

September 2011

CERTIFICATION OF ORIGINALITY

This is to certify that I am responsible for the work submitted in this project, that the original work is my own except as specified in the references and acknowledgements, and that the original work contained herein have not been undertaken or done by unspecified sources or persons.

A handwritten signature in black ink, appearing to read 'A. Shakir', with a long horizontal stroke extending to the right.

Ahmad Shakir bin Aminudin

ACKNOWLEDGEMENT

In the name of Allah, The Most Gracious, The Most Merciful. Praise to Allah S.W.T by whose grace and sanction I manage to complete Final Year Project within time.

I would like to extend my sincere gratitude to my supervisor Dr. Saravanan Karuppanan who has given me advices, opinions and guides in completion of this project. Through his kindness and precious moment, I manage to face all the problems that been encountered during these whole period. Thank you again for the knowledge sharing.

Not forgetting to other lecturers of UTP especially from the Mechanical Engineering department, thanks for useful thoughts and assistance that help me a lot in completing this project.

Last but not least, to my parents and colleagues for the supports given during the completion of this project.

ABSTRACT

Failure due to corrosion defects has been the major problem in maintaining pipeline's integrity. The loss of metal due to corrosion usually results in localized pits with various depth and irregular shapes which occur on its external and internal surfaces. An interacting defect is one that is located sufficiently close and able to interact with neighboring defects in an axial or circumferential direction. The maximum allowable pressure that can be sustained in a pipeline with interacting defects is lower than it is in single defects due to interaction of neighboring defects. There are several methods available to assess the corrosion metal loss defects in order to evaluate Fitness-for-Services (FFS) of the corroded pipeline. In this study, finite element simulations will be carried out to determine the maximum allowable burst strength of corroded pipeline with interacting defects. The finite element analysis (FEA) results show that failure pressure of corroded pipeline with interacting defects are higher than empirical values gained from DNV-RP-F101 Code,

TABLE OF CONTENTS

CERTIFICATION OF APPROVAL.								i
CERTIFICATION OF ORIGINALITY.								ii
ABSTRACT								iii
ACKNOWLEDGEMENT								iv
CHAPTER 1:	INTRODUCTION							1
	1.1.	Background of Study						1
	1.2.	Problem Statements						2
	1.3.	Objectives and Scope of Study.						3
CHAPTER 2:	LITERATURE REVIEW							4
	2.1	Pipeline Corrosion						4
	2.2	Interacting Defects						4
	2.3	Offset Defects						7
	2.4	Finite Element Analysis.						8
CHAPTER 3:	METHODOLOGY							10
	3.1.	Research Methodology.						10
	3.2	DNV-RP-F101						11
	3.3	Modeling in ANSYS						12
		3.3.1 Defining element types						12
		3.3.2 Defining material properties						13
		3.3.3 Creating model geometry						14
		3.3.4 Meshing						15
		3.3.5 Load						16
		3.3.6 Analysis.						17
		3.3.7 Comparison of Results						18
	3.4	Project Gantt chart						19

CHAPTER 4:	RESULTS AND DISCUSSIONS.	20
4.1	DNV Code Results	20
4.1.1	Allowable Corroded Pressure for Single Defects, p_1 and p_2	21
4.1.2	Allowable Corroded Pressure for Interacting Defects, P_{nm}	21
4.1.3	Maximum Allowable Corroded Pressure, p_{corr}	23
4.2	Overall Result Summary.	24
CHAPTER 5:	CONCLUSION AND RECOMMENDATION.	34
5.1	Conclusion	34
5.2	Recommendation	34
REFERENCES		35

LIST OF FIGURES

Figure 2.1 : Combined length of all combination of adjacent defects.	6
Figure 2.1 : Projection of overlapping defects onto a single projection line	8
Figure 3.1 : Process flow of the project	10
Figure 3.2 : Defining the element types of model	12
Figure 3.3 : Defining nonlinear properties of model	13
Figure 3.4 : Engineering Stress vs. Strain graph for X65.	13
Figure 3.5 : Creating model by partial annulus on workplane	14
Figure 3.6 : Half of the pipe with defect	15
Figure 3.7 : Mapped mesh of the pipe	15
Figure 3.8 : Symmetry Boundary Conditons of the model.	16
Figure 3.9 : Fixed end at all DOF (enclosed end)	16
Figure 3.10 : Internal load applied on pipe model	17
Figure 3.11 : Contour plot of Von Mises Stress distribution along the pipe	17
Figure 4.1 : Graph of Normalized corroded pressure, P_{corr} (MPa) / P_{intact} (MPa) vs spacing per square root of unit depth with thickness, $\frac{s}{\sqrt{D \times t}}$, for $d/t = 0.1$	25
Figure 4.2 : Graph of Normalized corroded pressure, P_{corr} (MPa) / P_{intact} (MPa) vs spacing per square root of unit depth with thickness, $\frac{s}{\sqrt{D \times t}}$, for $d/t = 0.2$	25
Figure 4.3 : Graph of Normalized corroded pressure, P_{corr} (MPa) / P_{intact} (MPa) vs spacing per square root of unit depth with thickness, $\frac{s}{\sqrt{D \times t}}$, for $d/t = 0.3$	26
Figure 4.4 : Graph of Normalized corroded pressure, P_{corr} (MPa) / P_{intact} (MPa) vs spacing per square root of unit depth with thickness, $\frac{s}{\sqrt{D \times t}}$, for $d/t = 0.4$	27
Figure 4.5 : Graph of Normalized corroded pressure, P_{corr} (MPa) / P_{intact} (MPa) vs spacing per square root of unit depth with thickness, $\frac{s}{\sqrt{D \times t}}$, for $d/t = 0.5$	27
Figure 4.6 : Graph of Normalized corroded pressure, P_{corr} (MPa) / P_{intact} (MPa) vs spacing per square root of unit depth with thickness, $\frac{s}{\sqrt{D \times t}}$, for $d/t = 0.6$	28
Figure 4.7 : Graph of Normalized corroded pressure, P_{corr} (MPa) / P_{intact} (MPa) vs spacing per square root of unit depth with thickness, $\frac{s}{\sqrt{D \times t}}$, for $d/t = 0.7$	29
Figure 4.8 : Graph of Normalized corroded pressure, P_{corr} (MPa) / P_{intact} (MPa) vs spacing per square root of unit depth with thickness, $\frac{s}{\sqrt{D \times t}}$, for $d/t = 0.8$	29
Figure 4.9 : Graph of Normalized corroded pressure, P_{corr} (MPa) / P_{intact} (MPa) vs spacing per square root of unit depth with thickness, $\frac{s}{\sqrt{D \times t}}$, for the FEA result	30

Figure 4.10 : Graph of Ratio of FEA over DNV Code vs depth per unit thickness. . . . 31

Figure 4.11 : Element solution of Von Misses stress distribution for $d/t = 0.2$,
 $\frac{s}{\sqrt{D \times t}} = 0.5$ (Internal view) 32

Figure 4.12 : Element solution of Von Misses stress distribution for $d/t = 0.2$,
 $\frac{s}{\sqrt{D \times t}} = 0.5$ (External view) 32

Figure 4.13: Closed view on the defect area for $d/t = 0.2$ and $\frac{s}{\sqrt{D \times t}} = 0.5$ 33

LIST OF TABLES

Table 3.1 : The analysis matrix.	18
Table 3.1 : Final Year Project 1 Gantt chart.	19
Table 3.2 : Final Year Project 2 Gantt chart.	19
Table 4.1 : Parameters of Sample with $d_1/t = d_2/t = 0.3$ and $\frac{s}{\sqrt{D \times t}} = 0.5$	30
Table 4.2 : Overall Result Summary.	34

CHAPTER 1

INTRODUCTION

Pipeline systems are generally a convenient means for transferring oil and gas onshore or offshore due to the economic and safety reasons. However, with increasing age, the pipeline integrity can be affected by a range of corrosion mechanism.

Pipeline is exposed to both internal and external corrosion. The internal corrosion of pipeline is due to the harsh condition of hydrocarbon fluid; the presence of CO₂, H₂S, organic acid and etc. While external corrosion occurs due to extreme condition of the surrounding environment in the event of failed preventive measures; older, degraded coat, or poorly coated pipeline ^[1, 2]. This will result in metal loss at corroded location in the pipeline and eventually may lead to its failure. The structural integrity assessment of corroded pipeline has become vital and the main interest to assist engineers to take wise decision toward replacing or repairing a pipeline. It is essential to ensure the continued safe operation and non hazardous occurrences which might affect the life and the environment.

1.1 Background of study

An interacting defect is defined as the one that interacts with neighboring defects in an axial or circumferential direction ^[3]. As the extent of space between corrosion defects decrease up to certain distance, they will begin to interact reducing the maximum allowable pressure that can be sustained in a pipeline. The objective of this project is to estimate the burst pressure of corroded pipeline due to interacting corrosion defects by the means of FEA. The analysis is performed by nonlinear FEA simulation using ANSYS Software. This project will study on the effect of different spacing between two defects aligned in longitudinal direction and their failure pressure. Then the results of the FEA will be compared to the numerical values gained from the DNV RP-F101 code.

1.2 Problem Statement

The impact of corroded pipeline problems cause economic consequences; reduced operating pressure, loss of production due to downtime, repairs or replacement, and consequently increase of costs. Thus, there are several pipelines systems kept in operation even though they have shown signs of corrosion based on the data obtain from the corrosion management, inspection, and monitoring system (i.e.: intelligent pig). The continued operations of these pipelines are basically after determining the FFS assessment for their residual strength and recalculating the maximum allowable internal pressure of the product being transferred ^[4]. The effect of pipeline burst strength of interacting defects will be lower than it is in single defects. A more reliable defect assessment method is needed due to the conservatism involved in the available assessment method ^[5]. This is an approach to understand the effect of interacting defects toward the pipeline burst strength in a more reliable and convenient method other than performing the experimental testing. Therefore, the modeling of the problem using the FEA method can assist engineers to assess the burst strength of pipeline with interacting defects.

1.3 OBJECTIVE AND SCOPE OF STUDY

The objectives of this project are:

- To assess the burst strength of corroded pipelines due to interacting defects.
- To compare the results from FEA with numerical values obtained from the available codes.

The scope of this project will be simplified as follows:

- The material of the pipelines is API 5L X65.
- Results from FEA will be compared with empirical solutions provided by DNV-RP-F101 code.
- The pipelines will be subjected to internal pressure only.

CHAPTER 2

LITERATURE REVIEW

2.1 Pipeline Corrosion

Unprotected pipelines are subjected to corrosion as well as when their corrosion preventions failed. Corrosion is defined as the destruction or deterioration of a material because of its reaction with the environment ^[6]. Corrosion defects in pipelines are assessed as metal loss defects that occur on the interior or exterior of pipeline surfaces. And if no appropriate maintenance actions taken, the location of corrosion become deteriorate. This consequently reduce the structural integrity of the pipeline hence can cause catastrophic failure of the system ^[7]. For many years, various methods for assessing pipeline corrosion are available and commercially have been practiced by the industry; such as ANSI/ASME B31G ^[8]. For more realistic way of pipeline corrosion representation ^[9], new criteria are developed, such as RSTRENG Effective Area ^[10], and DNV RP-F101 ^[3]. These methods include the specification dealing with the effects of the interacting defects. Even though these codes have been used widely for assessing the integrity of in-service pipelines, they are known to be conservative ^[11]. Meaning that, pipelines which have been assessed by these codes for the purpose of FFS analysis probably lead to either unnecessary maintenance or premature replacement.

2.2 Interacting Defects

The occurrence of corrosion is divided into several categories; individual pits, colonies of pits, general wall-thickness reduction, or in combinations ^[12]. For colonies of corrosion defects, as the distance between the defects decreases, they will begin to interact and resulting in reduced burst strength of the pipe. DNV-RP-F101 method for interacting defects (part A) will be used in this study to estimate the burst pressure of the corroded pipeline. In DNV procedure, all the defects that are supposed to interact are

projected onto a longitudinal line. The metal loss is represented by the maximum defects depth and the projected defects length.

In the case of overlapped defects, they are combined to form composite defect. The formation of combined defects is estimated by taking the combined length and the depth of the deepest defect. For combination of overlapping internal and external defect, the depth of the composite defect is the sum of maximum depth of those two defects.

Each defect or composite defects (i) with length (l_i) and depth (d_i) is treated as a single defect and failure pressure (p_i) is defined based on the expression below:

$$p_i = \gamma_m \frac{2t f_u (1 - \gamma_d (d_i/t)^*)}{(D-t) \left(1 - \frac{\gamma_d (d_i/t)^*}{Q_i} \right)} \quad i = 1, \dots, N \quad (2.1)$$

where N is the is number of projected defects, D is the nominal outside diameter (mm), t is uncorroded measured pipe wall thickness or t_{nom} (mm), f_u is the ultimate tensile strength, γ_d is the partial safety factor for corrosion depth and Q_i is the length correction factor for individual defect, given by:

$$Q_i = \sqrt{1 + 0.31 \left(\frac{l_i}{\sqrt{Dt}} \right)^2} \quad (2.2)$$

The correction depth over thickness ratio is determined by the following expression:

$$(d_i/t)^* = (d_i/t)_{meas} + \epsilon_d StD (d_i/t) \quad (2.3)$$

f_u = Minimum yield strength of the material

γ_m = Partial safety factor for model prediction

γ_d = Partial safety factor for corrosion depth

ϵ_d = Factor for defining fractile value for the corrosion depth

$StD[d/t]$ = Standard deviation of the measured (d/t) ration

Next, the combinations of adjacent defects are investigated. Take note that for combined defects; the effective length (l_{nm}) is the total length of the projected defects and the spacing between the defects (Figure 2.2). For defects from n to m , the effective length is given by

$$l_{nm} = l_m + \sum_{i=n}^{i=m-1} (l_i + s_i) \quad n, m = 1, \dots, N, \quad (2.4)$$

where s_i is the projected distance between the two adjacent defects.

Meanwhile, the effective depth (d_{nm}) of combined defect formed from all of interacting defects from n to m (Figure 2.1) is calculated as below:

$$d_{nm} = \frac{\sum_{i=n}^{i=m} d_i l_i}{l_{nm}} \quad (2.5)$$

The failure pressure (p_{nm}) of the combined defects from n to m is calculated by replacing (l_i) and (d_i) with (l_{nm}) and (d_{nm}) in Eqs. (2.1) and (2.2) respectively.

Where the abbreviations are represented by the following:

l_{nm} = Total longitudinal length of a defect combined with the adjacent defects n to m including spacing in between them (mm).

l_n = Longitudinal length of an individual defect (mm).

s_n = Longitudinal spacing between adjacent defects (mm).

d_n = Depth of corroded region (mm).

The minimum value, calculated for all single and combined defects, is taken as the failure pressure for the current projection line.

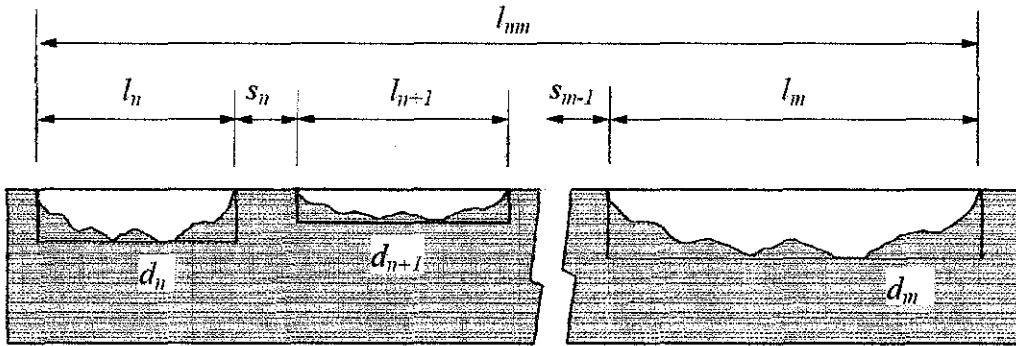


Figure 2.1: Combined length of all combination of adjacent defects

According to the DNV interaction rules, there is no interaction if the longitudinal (s_l) and circumferential (s_c) distances between defects satisfy the following conditions:

$$s_l > 2.0 \sqrt{Dt}$$

$$s_c > \pi \sqrt{Dt}$$

2.3 Offset Defects

In real life problem, the corrosion does not occur rigidly in one location on the wall of the pipeline, instead, the corrosion attack the surface randomly which create colony of defects that are scattered on the attacked location. The defects in the colony may be overlapped or offset to one another. According to DNV code, simplification had been made for cases of multiple defects which were overlapped or offset conditions. The overlapped defects are combined together to form composite defect. This composite defect is projected onto a single projection line (Figure 2.2).

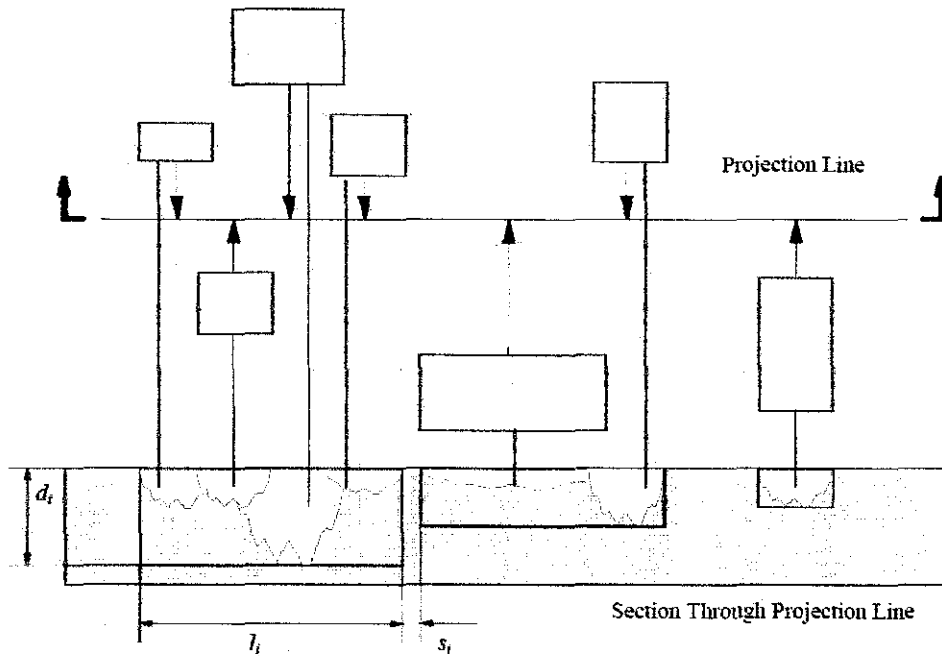


Figure 2.2: Projection of overlapping defects onto a single projection line

The simplification made on the DNV code does not take into consideration the offset condition of the interacting defect. In other word, the effect of offset between the interacting defects is negligible in the DNV calculation.

2.4 Finite Element Analysis

The FEM is a powerful technique to simulate the linear and nonlinear behavior of structures. In order to have this method to be able to correctly evaluate the corroded pipe, appropriate failure criterion should be established to decide the failure point during the simulation ^[5]. Research was done by Lee *et. al* ^[12] to predict the failure pressure for multiple corroded defects on gas pipeline made of API 5L X65 steel by means of burst testing and FEM. 3D-elastic plastic finite element simulation has been performed using ABAQUS. Multiple corrosion defects were conceived as pits with equal profile defects with size of length (50mm), width (50mm), and depth (8.75mm). These defects were aligned in longitudinal and circumferential directions. From the findings, comparison

between the burst tests and the finite element predictions showed that burst pressure had decreased with increased number of pits for longitudinal aligned defects. As for circumferential aligned defects, no significant change in burst pressure as distance between defects change.

Another study done by Silva *et. al* ^[9] on the assessment of pipe with interacting defects by FEM and neural networks application. The neural network is a mathematical algorithm which enables to relate the inputs and outputs parameters to establish the standard procedure for that particular process. The results from the finite element simulation were utilized as the databases for the neural networks system. The material been used was API 5L X52 steel. The defects are represented by two equally shaped defects of 80 mm x 32 mm with varied defect depth and separated by different defect spacing. These defects were aligned in longitudinal and circumferential directions. The results from the study showed that for case of longitudinal direction, specifically for closely space defect, relative pipe pressure capacity (ratio between failure pressure of multiple defect and single defect) reduced as depth of defect increased. On the contrary, for case of circumferential direction, little interaction of defects was observed which gave insignificant impact on the relative pipe pressure capacity.

CHAPTER 3

METHODOLOGY

3.1 Research Methodology

This project will be based on the following process flow (Figure 3.1). The methodology has been designed to fully optimise the time frame provided in order to completely carry out the planned and anticipated project works.

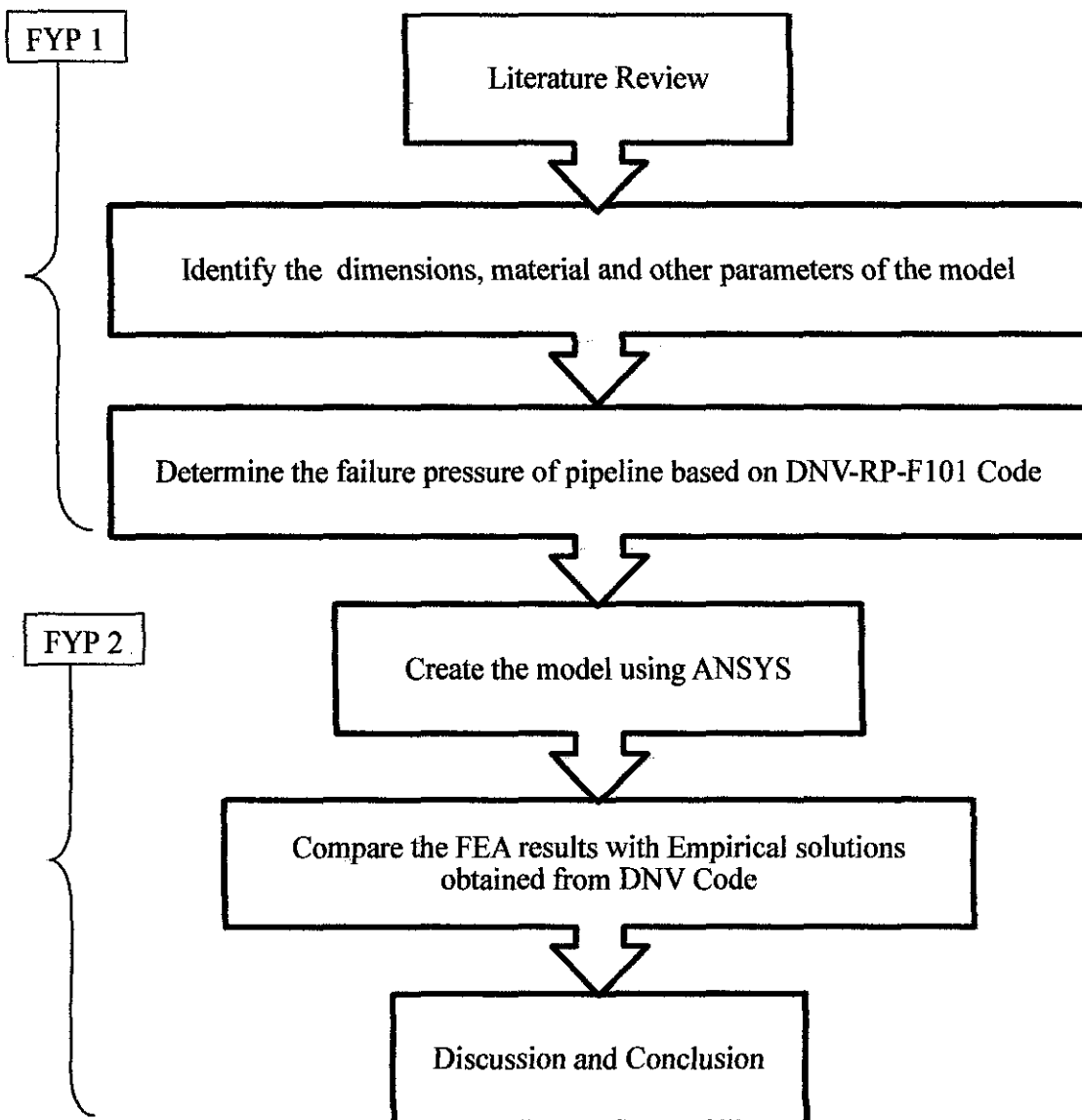


Figure 3.1: Process flow of the project

3.2 DNV-RP-F101

Firstly, the empirical correlation provided in DNV-RP-F101 code is studied. The related parameters such as depth of defects, spacing between defects, diameter of the pipeline, and length of the defects are determined by manipulating the correlation. The allowable corroded pressure of interacting defects is estimated using the following procedure:

- 3.1.1 The length of the defect is determined from the ratio between defect length and diameter of pipeline, l/D .
- 3.1.2 The allowable pipe corroded pressure ($p_1, p_2...p_N$) of each defect, or combined defect is calculated by using equation (2.1). The length correction factor is calculated based on equation (2.2). The failure pressure of the single defect will be chosen as the reference pressure.
- 3.1.3 The length between the defects is determined from the ratio between spacing of the defects and square root of diameter and thickness of the pipe, $\frac{s}{\sqrt{D \times t}}$.
- 3.1.4 Afterward, all combinations of adjacent defects are calculated. The combined length is calculated using equation (2.4).
- 3.1.5 Then, the effective depth of the combined defects is calculated based on equation (2.5).
- 3.1.6 The allowable corroded pipe pressure of the combined defect (p_{nm}) is determined from equation (2.1) by replacing (l_i) and (d_i) with (l_{nm}) and (d_{nm}) in equation (2.1) and (2.2) respectively. The term (d_i) in equation (2.3) is replaced with (d_{nm}).

Several assumptions have been made in this study, firstly, the length of both defects that are supposed to interact are equal. Secondly, the interacting defects are considered between defects with similar depth only.

3.3 Modeling in ANSYS

After conducting the analysis using DNV RP-F101 code, finite element models are developed using ANSYS, a well known engineering simulation software. The loading involved in this simulation is distributed internal pressure loading. The purpose of this analysis is to estimate the corroded pipe pressure.

3.3.1 Defining element types

The ANSYS element library contains more than 100 different element types. Each element type has a unique number and a prefix that identifies the element category. The element type determines whether the element lies in two-dimensional or three-dimensional space and the degree-of-freedom set (which in turn implies the discipline - structural, thermal, magnetic, electric, quadrilateral, brick, etc.). In this project, for the pipe steel X65, SOLID95 is used to analyse the 3D models. The element is defined by 20 nodes having three degrees of freedom at each node, which is translations in the nodal x, y, and z directions. The element is applicable for mapped meshing (controlled meshing). It can tolerate irregular shapes without as much loss of accuracy and have compatible displacement shapes and are well suited to model curved boundaries.

Main Menu > Preprocessor > Element Type > Add / Edit / Delete (Figure 3.2)

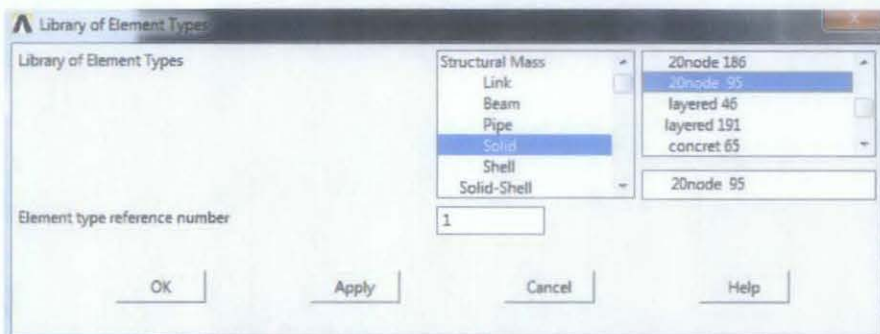


Figure 3.2: Defining the element types of model

CHAPTER 4

RESULTS AND DISCUSSIONS

4.1 DNV Code Results

The calculation is based on assessment of interacting defects (Calibrated safety factor, Part A). The parameters of pipe steel X65 that will be used in the calculation is stated as in Table 4.1.

Table 4.1: Parameters of Sample with $d_1/t = d_2/t = 0.3$ and $\frac{s}{\sqrt{D \times t}} = 0.5$

Parameter	Value
Thickness, t (mm)	20
Diameter, D (mm)	300
Defects Length, $l_1 = l_2$ (mm)	100
Width of corroded region c (mm)	90
Safety Factor for Model, γ_m	0.72
Tensile Strength, f_u (MPa)	530.9
Fractile value for corrosion depth, \mathcal{E}_d	1
Safety Factor for Corrosion Depth, γ_d	1.28
Depth, $d_1 = d_2$ (mm)	6
Spacing, s (mm)	38.73

4.1.1 Allowable Corroded Pressure for Single Defects, p_1 and p_2

1. Length Correction Factor, Q_1

$$\begin{aligned} Q_1 &= \sqrt{1 + 0.31 \left(\frac{l_1}{\sqrt{Dt}} \right)^2} \\ &= \sqrt{1 + 0.31 \left(\frac{100 \text{ mm}}{\sqrt{300 \text{ mm} \times 20 \text{ mm}}} \right)^2} \\ &= \mathbf{1.231} \end{aligned}$$

2. Allowable corroded pressure, p_1 and p_2

$$\begin{aligned} p_1, p_2 &= \gamma_m \frac{2t f_u (1 - \gamma_a (d_1/t)^*)}{(D-t) \left(1 - \frac{\gamma_a (d_1/t)^*}{Q_1} \right)} \\ &= \frac{0.72 \times 2 \times 20 \times 530.9 \times (1 - 1.28(0.38))}{(300 - 20) \left(1 - \frac{1.28(0.38)}{1.231} \right)} \\ &= \mathbf{46.37 \text{ MPa}} \end{aligned}$$

4.1.2 Allowable Corroded Pressure for Interacting Defects, p_{nm}

1. Total length, l_{nm}

$$\begin{aligned} l_{nm} &= l_m + \sum_{i=n}^{i=m-1} (l_i + s_i) \\ &= (100 + 100 + 38.73) \text{ mm} \\ &= \mathbf{238.73 \text{ mm}} \end{aligned}$$

2. Effective Depth, d_{nm}

$$d_{nm} = \frac{\sum_{i=n}^{i=m} d_i l_i}{l_{nm}}$$
$$= \frac{(6\text{mm} \times 100\text{mm}) + (6\text{mm} \times 100\text{mm})}{238.73\text{mm}}$$
$$= \mathbf{5.027\text{mm}}$$

3. Length Correction Factor, Q_{nm}

$$Q_{nm} = \sqrt{1 + 0.31 \left(\frac{l_{nm}}{\sqrt{Dt}} \right)^2}$$
$$= \sqrt{1 + 0.31 \left(\frac{238.73\text{mm}}{\sqrt{300\text{mm} \times 20\text{mm}}} \right)^2}$$
$$= \mathbf{1.986}$$

4. Adjusted depth ratio, $(d_{nm}/t)^*$

$$(d_{nm}/t)^* = (d_{nm}/t)_{meas}$$
$$= \left(\frac{5.027}{20.00} \right)$$
$$= \mathbf{0.251}$$

5. Allowable corroded pressure, p_{nm}

$$\begin{aligned} p_{nm} &= \gamma_m \frac{2t f_u (1 - \gamma_a (d_{nm}/t)^*)}{(D-t) \left(1 - \frac{\gamma_a (d_{nm}/t)^*}{Q_{nm}} \right)} \\ &= \frac{0.72 \times 2 \times 20.00 \times 530.9 \times (1 - 1.28(0.251))}{(300 - 20) \left(1 - \frac{1.28(0.251)}{1.986} \right)} \\ &= \mathbf{44.199 \text{ MPa}} \end{aligned}$$

4.1.3 Maximum Allowable Corroded Pressure, p_{corr}

$$p = \min(p_l, p_{nm})$$

$$= \mathbf{44.199 \text{ MPa}}$$

4.2 Overall Result Summary

The overall results summary of empirical solution and FEA non-linear analysis for X65 steel are tabulated in Table 4.2. The stopping criterion used in FEA is when the Von-Mises stress reaches the ultimate tensile stress across the entire ligament of the pipe.

Table 4.2 : Overall Result Summary

d/t	$\frac{s}{\sqrt{D \times t}}$	DNV code	FEA
0.1	0.5	51.53	77.70
	1.0	51.71	77.90
	2.0	52.04	78.00
	4.0	52.56	78.40
	8.0	53.18	79.20
0.2	0.5	48.09	71.52
	1.0	48.55	71.94
	2.0	49.36	72.15
	4.0	50.46	73.02
	8.0	51.74	74.05
0.3	0.5	44.20	61.30
	1.0	45.09	62.50
	2.0	46.46	64.00
	4.0	48.30	66.70
	8.0	50.28	67.10
0.4	0.5	39.77	53.86
	1.0	41.28	55.81
	2.0	43.42	58.27
	4.0	46.08	61.32
	8.0	48.81	63.95
0.5	0.5	34.69	45.58
	1.0	37.08	49.30
	2.0	40.21	53.10
	4.0	43.79	56.10
	8.0	47.32	60.60
0.6	0.5	28.80	36.73
	1.0	32.42	40.66
	2.0	36.78	46.90
	4.0	41.44	52.58
	8.0	45.81	57.92
0.7	0.5	21.89	27.51
	1.0	27.22	34.13
	2.0	33.14	41.24
	4.0	39.02	49.66
	8.0	44.29	56.05
0.8	0.5	13.66	17.03
	1.0	21.37	26.84
	2.0	29.26	36.19
	4.0	36.54	45.52
	8.0	42.75	53.41

Generally, the overall results as stated in Table 4.2, show that the results obtained from FEA is higher compared to the values obtained using DNV Code. The non linear analysis yield results which are in similar trend with the empirical solution obtained from the DNV Code.

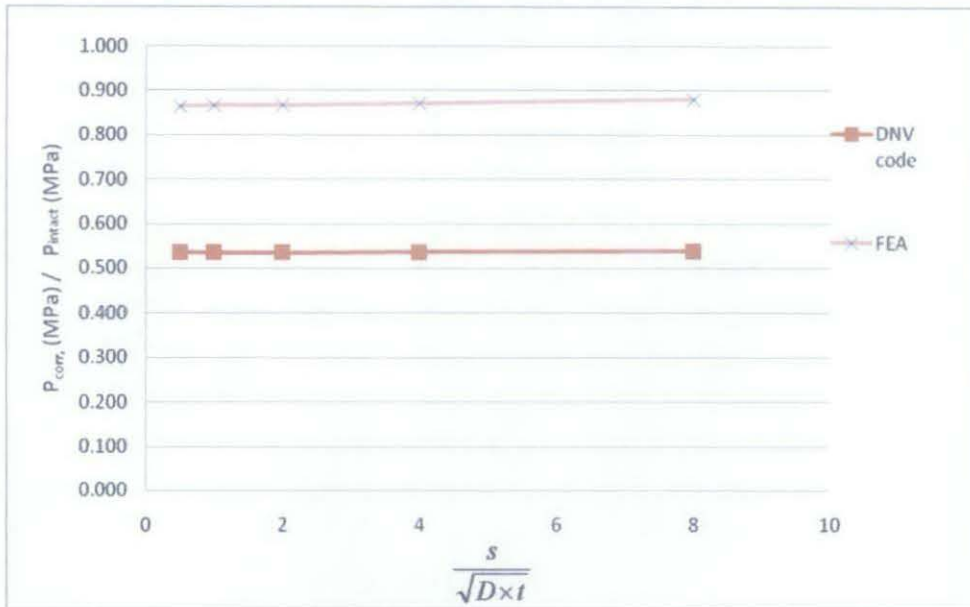


Figure 4.1: Graph of Normalized corroded pressure, P_{corr} (MPa) / P_{intact} (MPa) vs spacing per square root of unit depth with thickness, $\frac{s}{\sqrt{D \times t}}$, for $d/t = 0.1$

Figure 4.1 shows the comparison between the results from DNV Code and FEA for case $d/t = 0.1$. The graph shows that the effect of spacing between the defects does not differ much toward the failure pressure for both techniques. In other word, the effect of interaction for defects with depth of 10% of pipe wall thickness will not have significant impact toward the pipe failure pressure. The Ratio of FEA over DNV Code is 1.499.

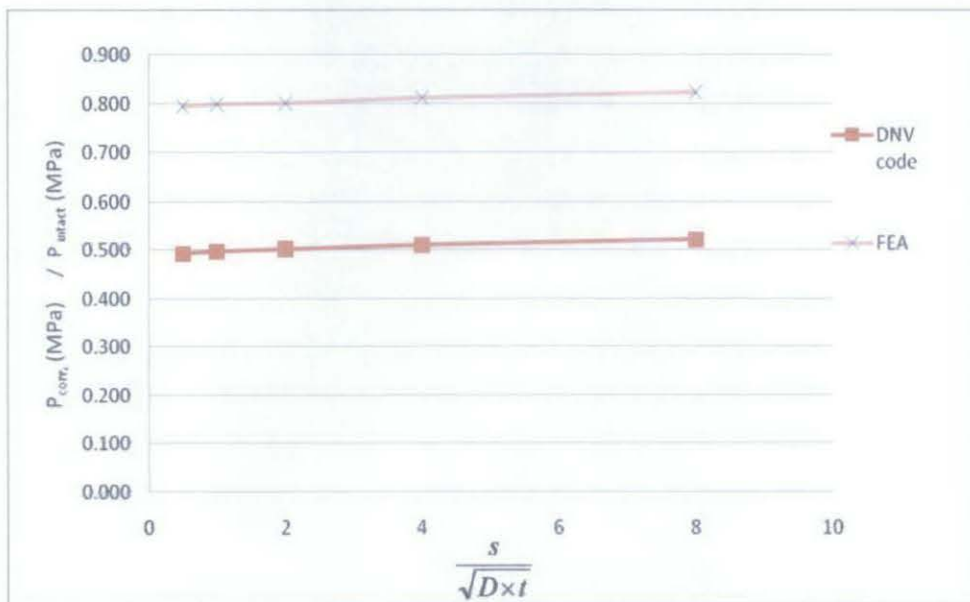


Figure 4.2: Graph of Normalized corroded pressure, P_{corr} (MPa) / P_{intact} (MPa) vs spacing per square root of unit depth with thickness, $\frac{s}{\sqrt{D \times t}}$, for $d/t = 0.2$

Figure 4.2 shows the comparison between the results from DNV Code and FEA for case $d/t = 0.2$. As the distance between the defects increase the failure pressure increase slightly. The interaction start to occur when the distance between the defects is small. However, for defect with depth of 20% of pipe wall thickness, it only experienced small interaction effect. Thus the failure pressure only has minor increment as the distance of the defects is increased. The ratio of FEA over DNV Code is 1.462.

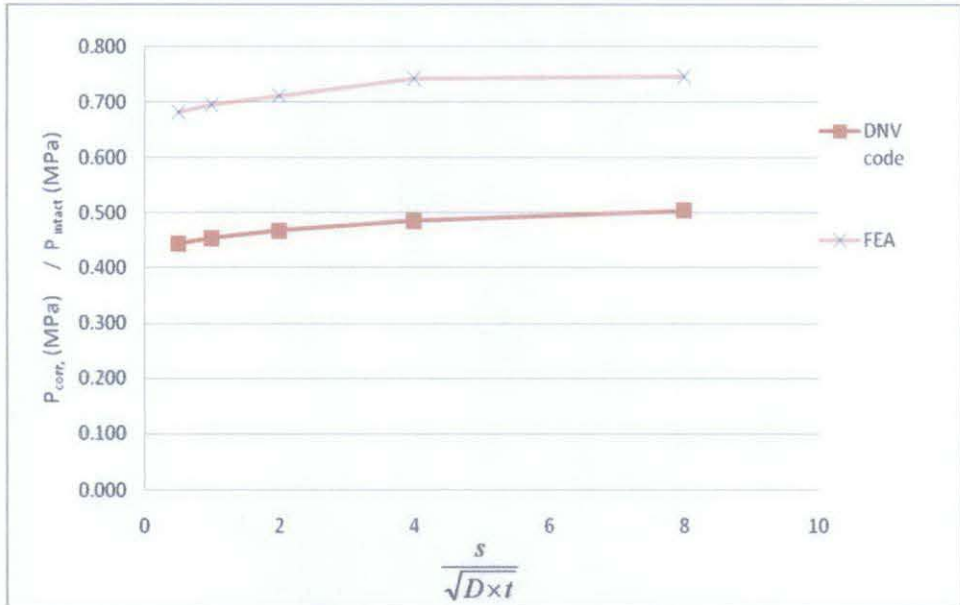


Figure 4.3: Graph of Normalized corroded pressure, P_{corr} (MPa) / P_{intact} (MPa) vs spacing per square root of unit depth with thickness, $\frac{s}{\sqrt{D \times t}}$, for $d/t = 0.3$

Figure 4.3 shows failure pressure comparison for case $d/t = 0.3$. The graph shows that the failure pressure is lower when the distance between defects is small and as the distance between the defects increase up to $\frac{s}{\sqrt{D \times t}} = 4$ the failure pressure increase significantly. For $\frac{s}{\sqrt{D \times t}} > 4$, the failure pressure increase with small amount. The effect of interaction is significant when the distance is small and later the effect of interaction is small as spacing between defects is far from each other. Defects with depth of 30% of pipe wall thickness will show significant interaction effect when the distance between defects is small, $\frac{s}{\sqrt{D \times t}} < 4$. The ratio of FEA over DNV Code is 1.373.

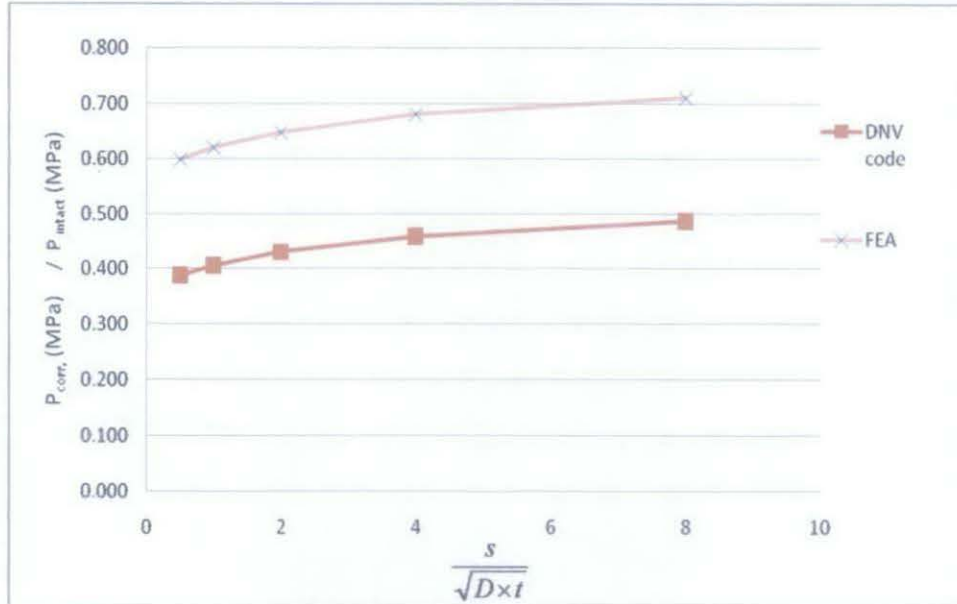


Figure 4.4: Graph of Normalized corroded pressure, P_{corr} (MPa) / P_{intact} (MPa) vs spacing per square root of unit depth with thickness, $\frac{s}{\sqrt{D \times t}}$, for $d/t = 0.4$

Figure 4.4 shows failure pressure comparison for case $d/t = 0.4$. The graph shows that the initial failure pressure is lower and as the distance between the defects increases the failure pressure increase. For defects with depth of 40% of pipe wall thickness, the interaction effect is high when the distance between defects is small and the effect gradually decreases as the distance is increased, resulting increased failure pressure. The ratio of FEA over DNV Code is 1.338.

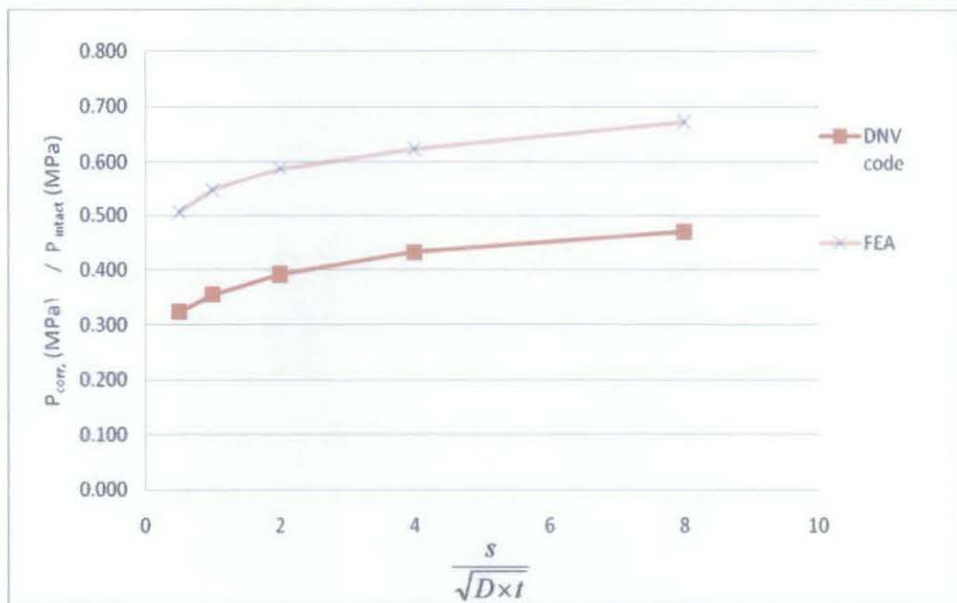


Figure 4.5: Graph of Normalized corroded pressure, P_{corr} (MPa) / P_{intact} (MPa) vs spacing per square root of unit depth with thickness, $\frac{s}{\sqrt{D \times t}}$, for $d/t = 0.5$

Figure 4.5 shows failure pressure comparison for case $d/t = 0.5$. The graph shows that the initial failure pressure is lower and as the distance between the defects increases, the failure pressure increase. For defects with depth of 50% of pipe wall thickness, the interaction effect show similar pattern as for case $d/t = 0.4$ but the effect of interaction is increased. The difference in term of failure pressure is high between the small defects spacing and large defects spacing. The ratio of FEA over DNV Code is 1.305.

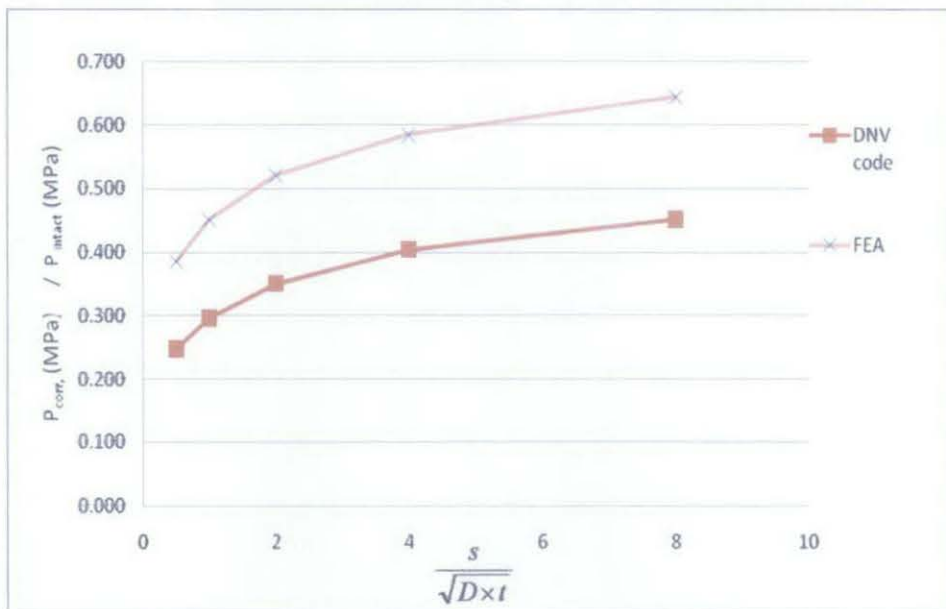


Figure 4.6: Graph of Normalized corroded pressure, P_{corr} (MPa) / P_{intact} (MPa) vs spacing per square root of unit depth with thickness, $\frac{s}{\sqrt{D \times t}}$, for $d/t = 0.6$

Figure 4.6 shows failure pressure comparison for case $d/t = 0.6$. The graph shows that failure pressure increase significantly as the distance between defects increased. For defects with depth of 60% of pipe wall thickness, the interaction effect is greater at small defects spacing resulting low failure pressure. Similar trend as from the previous case, the failure pressure increase as the distance between defects increased. The ratio of FEA over DNV Code is 1.267.

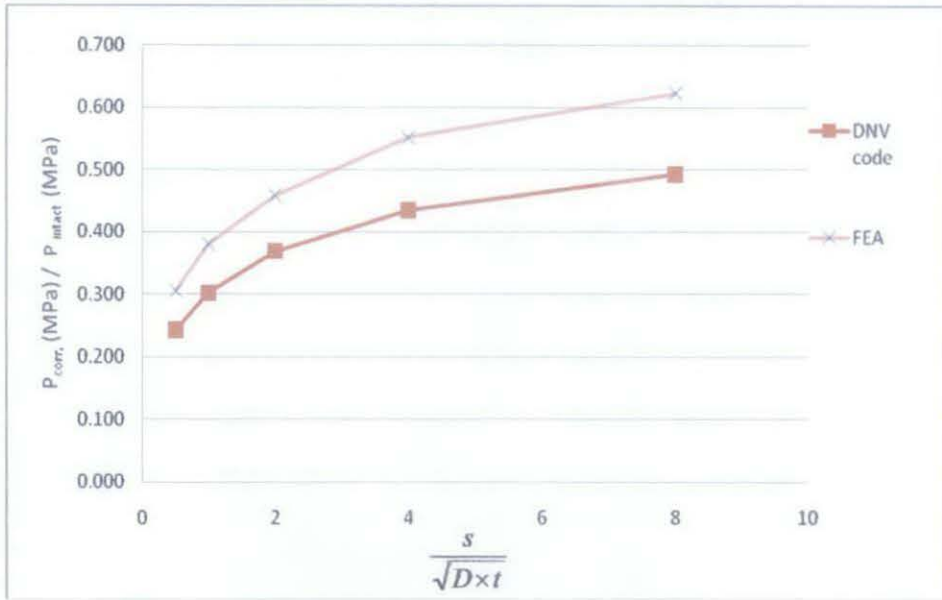


Figure 4.7: Graph of Normalized corroded pressure, P_{corr} (MPa) / P_{intact} (MPa) vs spacing per square root of unit depth with thickness, $\frac{s}{\sqrt{D \times t}}$ for $d/t = 0.7$

Figure 4.7 shows failure pressure comparison for case $d/t = 0.7$. The graph shows that failure pressure increase significantly as the distance between defects increased. For small defects spacing, the FEA result has small difference compared to the value DNV Code. But as the distance between defects increase, the difference between DNV Code and FEA is higher. For defects with depth of 70% of pipe wall thickness, the interaction effect is greater at small defects spacing resulting low failure pressure. The failure pressure increase drastically as the distance between defects increased. The ratio of FEA over DNV Code is 1.259.

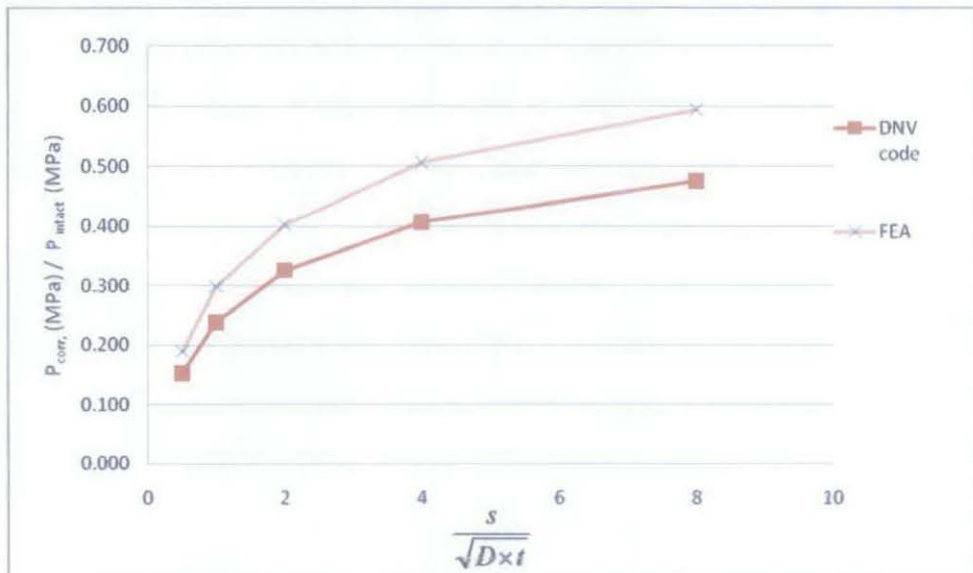


Figure 4.8: Graph of Normalized corroded pressure, P_{corr} (MPa) / P_{intact} (MPa) vs spacing per square root of unit depth with thickness, $\frac{s}{\sqrt{D \times t}}$, for $d/t = 0.8$

Figure 4.8 shows failure pressure comparison for case $d/t = 0.8$. The graph shows that failure pressure increase significantly as the distance between defects increased. For small defects spacing, the FEA result is approaching the DNV Code. The difference of failure pressure between DNV Code and FEA is small when the defect spacing is small. And as the distance increase, the failure pressure increase. For defects with depth of 80% of pipe wall thickness, the interaction effect is greater at small defects spacing resulting low failure pressure. For small defects spacing, even though the results yield from both method show nearly similar results but only with small difference, the value from FEA method is higher compared to DNV Code. The failure pressure increase drastically as the distance between defects increased. The ratio of FEA over DNV Code is 1.247.

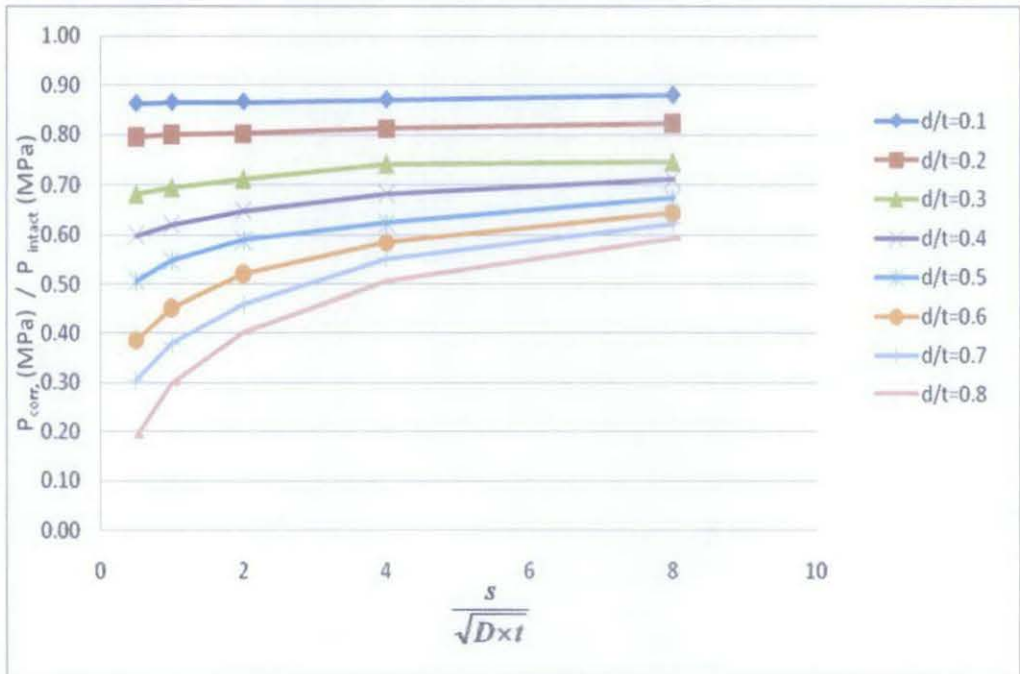


Figure 4.9: Graph of Normalized corroded pressure, P_{corr} (MPa) / P_{intact} (MPa) vs spacing per square root of unit depth with thickness, $\frac{s}{\sqrt{D \times t}}$, for the FEA result.

From the graph above, it is observed that as the distance between defects increase, the maximum allowable corroded pressure will increase. For defect with smaller depth, the failure pressure has no significant changes as the distance between defects increased. Meanwhile, defect with greater depth will result on large failure pressure increment as the distance between defects is increased.

Furthermore, as the depth of the defects increase, the failure pressure will decrease. The failure pressure at the small defects spacing reduced significantly and the effect of interaction is critical within this region. This shows that, when the spacing between the defects is small, they start to interact with each other and reduced the maximum allowable corroded pipe pressure.

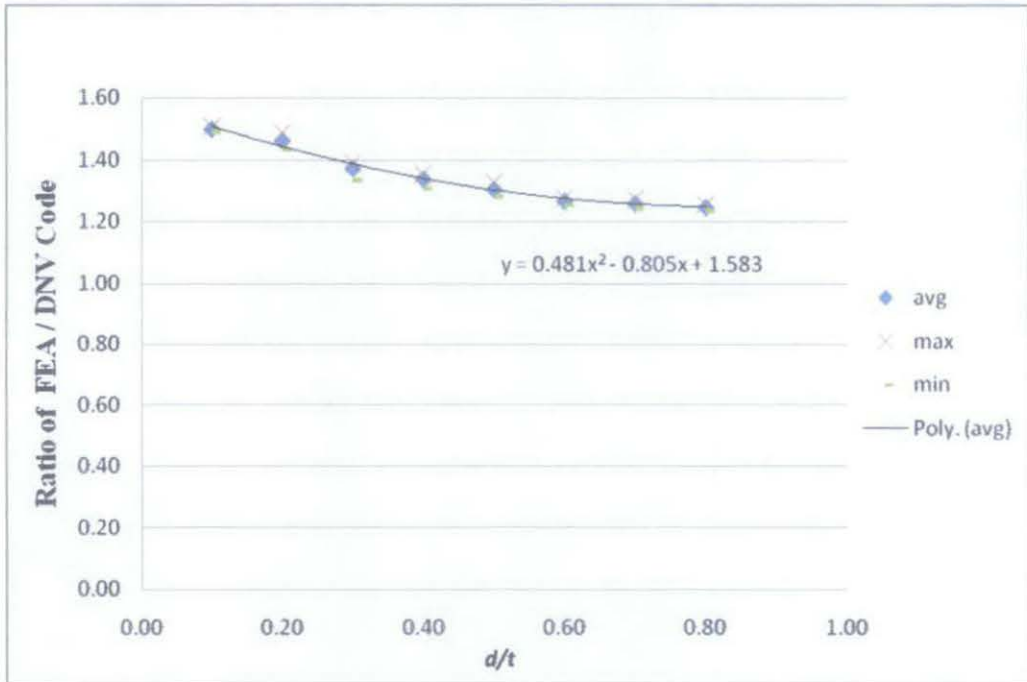


Figure 4.10: Graph of Ratio of FEA over DNV Code vs depth per unit thickness.

The result from FEA is always higher than DNV Code. This is due to safety factor applied in the empirical calculation which yields on lower corroded pipe failure pressure as to avoid reaching the exact failure pressure during standard operating condition. Figure 4.10 shows the factor of the ratio between FEA and DNV Code. The factor is not a fixed value since the multiplication factor is not the same for every cases of defects depth. This is due to stress concentration at the edges of the defects during the simulation process. The deeper the defect depth, the higher stress concentration occur at the edge of the defect. Since the remaining pipe wall thickness reduced, the stress distribution on the entire ligament of the edge easily reaches the failure criterion. From the graph above, it shows a decreasing trend as the depth of the defects is increasing. The best plot on the graph is based on the average value of the ratio of FEA over DNV Code. The factor can be expressed as a function of:

$$\text{Factor} = 0.481(d/t)^2 - 0.805(d/t) + 1.583.$$

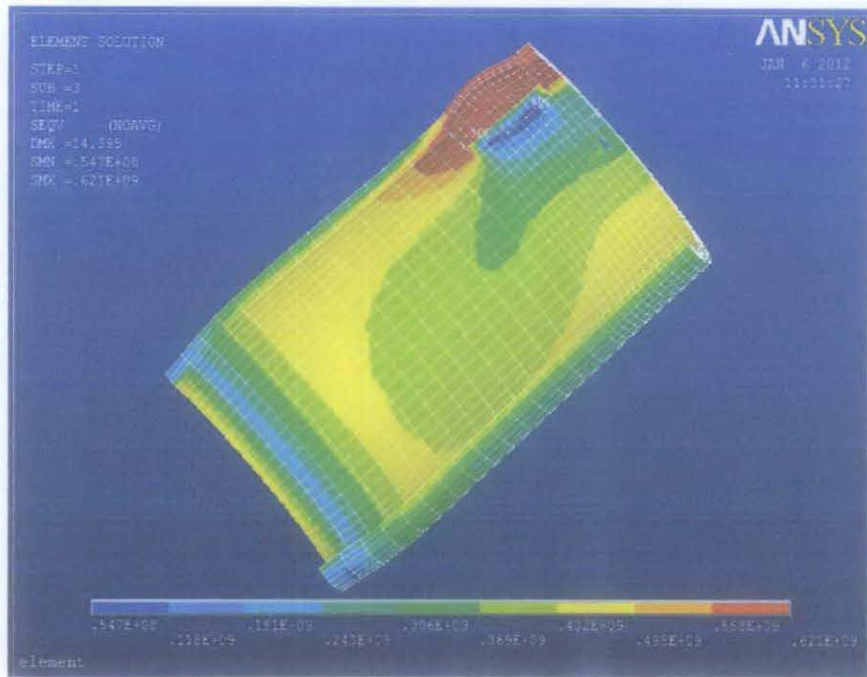


Figure 4.11: Element solution of Von Misses stress distribution for $d/t = 0.2$, $\frac{s}{\sqrt{D \times t}} = 0.5$ (Internal view)

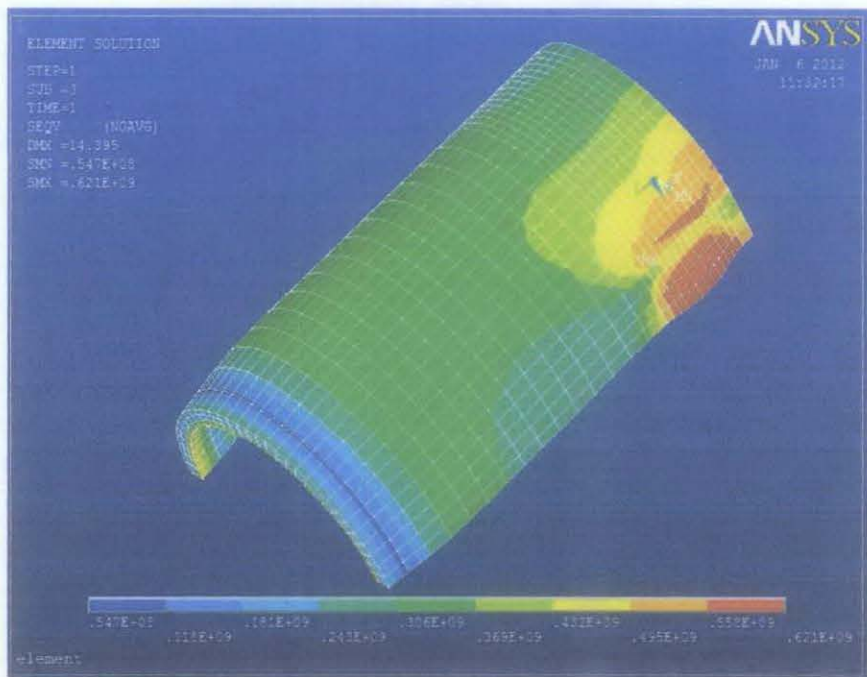


Figure 4.12: Element solution of Von Misses stress distribution for $d/t = 0.2$, $\frac{s}{\sqrt{D \times t}} = 0.5$ (External view)

Figure 4.11 and 4.12 show the element solution of the model for $d/t = 0.2$ and $\frac{s}{\sqrt{D \times t}} = 0.5$. The stopping criterion of the simulation is when the Von Misses stress distribution reaches the ultimate tensile strength ($\sigma_{UTS} = 530.9\text{MPa}$) across the entire thickness of the ligament.

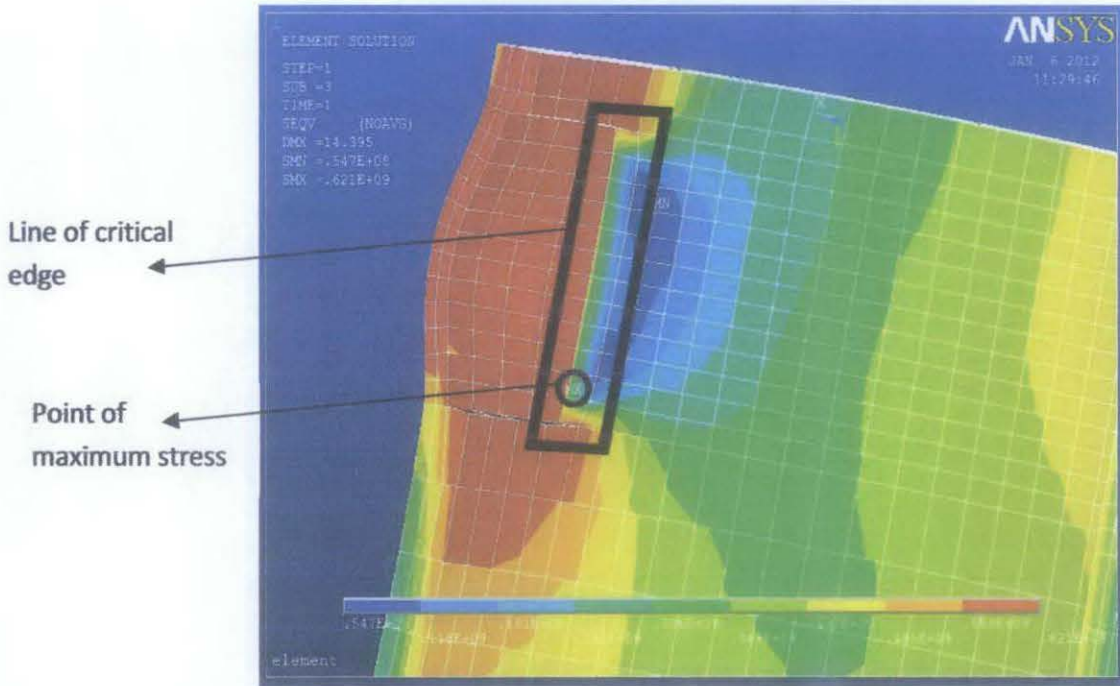


Figure 4.13: Closed view on the defect area for $d/t = 0.2$ and $\frac{s}{\sqrt{D \times t}} = 0.5$.

As the pressure applied on the internal surface of the pipe increased, the critical stress start to propagate along the edge of the defect and spread around the defect area. The assessment of the entire ligament is determined by consider the stress distribution across the thickness on several points at the critically defect area. Figure 4.13 shows the maximum stress point (MX) which occur at the edge of the defect. The stress distribution is analysed based on three points along the line of critical edge; the maximum stress point, middle point, and end point of the edge.

CHAPTER 5

CONCLUSION AND RECOMMENDATION

5.1 CONCLUSION

Consideration for maintenance or replacement of corroded pipeline is crucial because it affects directly to the cost of the firm. The available codes that are widely being used in the industry is too conservative. This may lead to unnecessary maintenance or premature replacement of corroded pipeline. Therefore, the FEA is one of the accurate methods to assess the burst strength of the corroded pipeline. Burst strength of pipeline with interacting corrosion defects can be accurately predicted by FEA using ANSYS software. The application of FEA can reduce the conservatism involved in the conventional methods. From this study, the ratio of FEA over DNV Code is a function of (d/t) given by: $\text{Factor} = 0.481(d/t)^2 - 0.805(d/t) + 1.583$.

5.2 RECOMMENDATION

Distance between defects is one of major factor toward the interaction to be occurred between defects. As the distance of the defect is increasing, the effect of interaction decrease and lead to increase in maximum allowable pipe failure pressure. In this study, it only sees the effect of interacting defects with similar defect depth. Further study can focus on the effect of interaction between defects with different depth.

REFERENCES

- [1] N. Shafiq, M.C. Ismail, Belachew C. T., K.Saravanan, and M.F. Nuruddin, 2010. Burst Test, Finite Element Analysis and Structural Integrity of Pipeline System. Hydrocarbon Asia's Engineering and Operations Convention, Kuala Lumpur, Malaysia.
- [2] B.A Chouchaoui and R.J Pick, 1996. Behavior of Longitudinal Aligned Corrosion Pits, *Int. J. Press. Ves. & Piping*, 67: 17-35.
- [3] DNV, Oct 2004. Recommended Practice DNV-RP-F101, Corroded Pipeline, Hovik, Norway. Pp 42.
- [4] T.A Netto, U.S. Ferraz, S.F Estefen, 2005. The Effect of Corrosion Defects on The Burst Pressure of Pipelines. *Journal of construction steel research*, 61: 1185-1204.
- [5] Belachew C. T., M. C. Ismail, and K.Saravanan, 2011. Burst Strength Analysis of Corroded Pipelines by Finite Element Method, *Journal of Applied sciences. Asian Network for Scientific Information*.
- [6] M. G. Fontana, 1987. *Corrosion Engineering*, Third Edition, Mc Graw-Hill, London. ISBN- 0-07-100360-6, p: 4.
- [7] Pipeline Corrosion, Public Affairs – White papers, Nace International
Retrieved from
<http://www.nace.org/content.cfm?parentid=1046¤tID=1424>
- [8] ANSI/ASME, 1991. *Manual for Determining the Remaining Strength of Corroded pipelines: A supplement to ASME B31 Code for Pressure Piping*. American Society of Mechanical Engineers, USA., pp 55.
- [9] R.C.C. Silva, J.N.C. Guerrero, A.F.D. Loula, 2007. A Study of Pipe Interacting Corrosion Defects using FEM and Neural networks, *Advance in Engineering Software*, 38: 868-875.

- [10] J.F. Kiefner and P.H. Vieth, 1989. A Modified Criterion for Evaluating the Remaining Strength of Corroded Pipe. Final report on Project PR 3-805, Pipeline Research Committee, American Gas Association.
- [11] Belachew, C.T., M.C. Ismail, and K.Saravanan, 2009. Capacity assessment of corroded pipelines using available codes. NACE Asia Pacific, Kuala Lumpur. Retrieved from http://eprints.utp.edu.my/1772/1/NACE_Conference_Paper.pdf
- [12] Y.K.Lee, Y.P. Lim, M.-W.Moon, W.H. Bang. K.H. Oh, W.-S. Kim, 2005. The prediction of failure pressure of gas pipeline with multi corroded region, Material Science Forum, Vol 475-479, p 3323-3326.